GFD 2013 Lecture 4: Shallow Water Theory

Paul Linden; notes by Kate Snow and Yuki Yasuda

June 20, 2014

1 Validity of the hydrostatic approximation

In this lecture, we extend the theory of gravity currents analysis by now applying the theory of the shallow water system. In the shallow water system, the hydrostatic approximation ($p_z = -\rho g$) and uniform motion with respect to height ($u_z = 0$) are assumed. Thus we have to check their validity.

First, in order to discuss the validity of the hydrostatic approximation, characteristic scales are introduced: L for horizontal length; U for horizontal velocity; H for vertical length; and W for vertical velocity. From the two dimensional incompressible condition $\frac{\partial u}{\partial x} + \frac{\partial w}{\partial z}$, $W \sim \epsilon U$ holds where $\epsilon := \frac{H}{L}$. By using the momentum equation in the x direction, the characteristic scale of pressure (P) can be estimated:

$$\underbrace{u_t}_{\frac{U}{T}} + \underbrace{uu_x + wu_z}_{\frac{U^2}{L}} = -\frac{1}{\rho}p_x, \tag{1}$$

$$P = \rho \ \max\left[\frac{UL}{T}, U^2\right]. \tag{2}$$

When the state is nearly steady [1], P is equal to ρU^2. Then the magnitude of each term in the vertical momentum equation can be estimated as follows:

$$\underbrace{uw_x + ww_z}_{\epsilon\frac{U^2}{L}} = \underbrace{-\frac{1}{\rho}p_z}_{\frac{U^2}{H}} - g. \tag{3}$$

Therefore, the magnitude of inertia terms are much smaller than that of the vertical pressure gradient, when the aspect ratio (ϵ) is small:

$$\frac{uw_x + ww_z}{-\frac{1}{\rho}p_z} = O(\epsilon^2). \tag{4}$$

This fact means that the hydrostatic balance holds with an accuracy of second order of ϵ.

Then it can be shown that the fluid layer moves uniformly in the z direction ($u_z = 0$) with the same accuracy. By differentiating (3) with respect to x, $p_{xz} = O(\epsilon^2)$ can be shown. Thus, if the fluid is initially uniform ($u_z|_{t=0} = 0$), uniformity also holds in later times with an accuracy of second order of ϵ.

[1] Or the time scale is equal to the advection time scale (L/U).

2 One layer shallow water equations

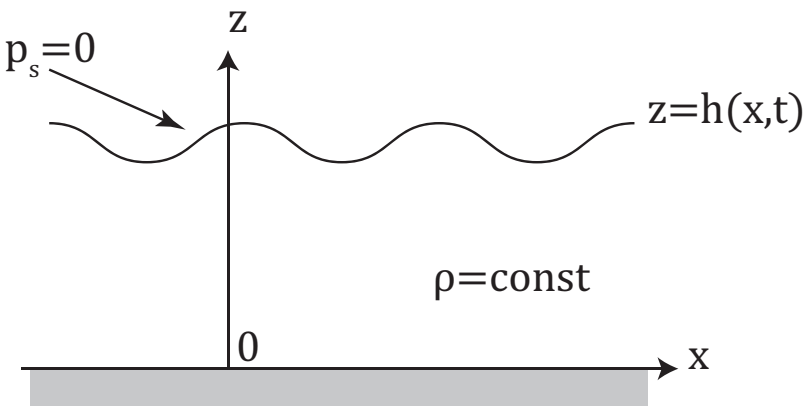

Figure 1: Two dimensional fluid system with a constant density. For simplicity, the pressure at the surface is taken to be zero.

We assume the following three things and then derive the one layer shallow water equations for the two dimensional fluid system with a constant density (Figure 1):

1. The hydrostatic balance holds.
2. Fluid moves uniformly with respect to height.
3. The aspect ratio is small.

Note that the third assumption is necessary for the validity of the other assumptions.

By the first assumption, p is equal to $\rho g\{h(x,t) - z\}$. By using the second assumption, the horizontal momentum equation becomes as follows:

$$u_t + uu_x = -gh_x. \tag{5}$$

By integrating the continuity equation and using the second assumption, the time evolution equation of h can be derived as follows:

$$\begin{aligned} w|_{z=h} &= -\int_0^h u_x dz, \\ \frac{Dh}{Dt} &= -hu_x. \end{aligned} \tag{6}$$

Note that the bottom boundary is flat, i.e., $w|_{z=0} = 0$, and the vertical variation of surface $\frac{Dh(x,t)}{Dt}$ is equal to $\frac{\partial h}{\partial t} + u\frac{\partial h}{\partial x}$. Thus (6) becomes

$$h_t = -\left(hu\right)_x. \tag{7}$$

The shallow water system consists of two equations (5), (7) and has two dependent variables $u(x,t), h(x,t)$.

When an axisymmetrical flow is considered, (7) becomes:

$$h_t + (uh)_r + \frac{uh}{r} = 0, \tag{8}$$

where r is radius, and u is radius velocity component. When the two layer stratified fluid [2] is considered as another extension, the interface of two layers is governed by (5) and (7), with g replaced by the reduced gravity (g').

3 Release in a channel

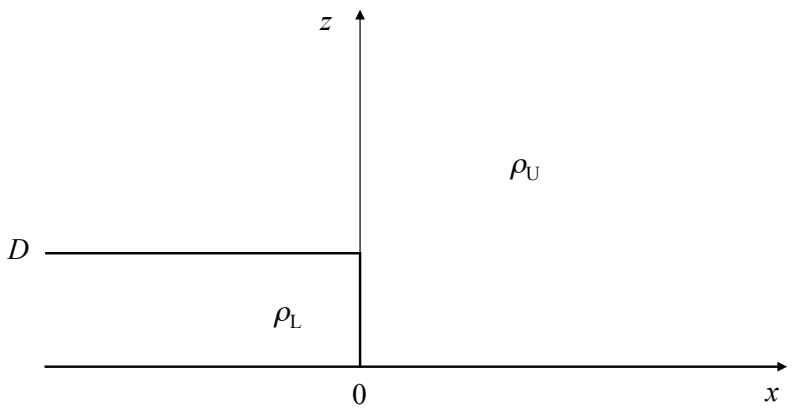

Figure 2: The initial state of gravity current.

Here, the gravity current is examined as an interface of the two layer shallow water system (Figure 2). Note that the mixing of the two different densities is not considered, and so g' is constant. The governing equations are the following:

$$u_t + uu_x + 2cc_x = 0, \tag{9}$$

$$(2c)_t + u(2c)_x + cu_x = 0, \tag{10}$$

where $c := \sqrt{g'h}$ is the phase speed of long waves. The initial conditions are then given by:

$$u(x,0) = 0(-\infty < x < \infty), \tag{11}$$

$$h(x,0) = \begin{cases} D & (x < 0), \\ 0 & (x > 0). \end{cases} \tag{12}$$

Further two conditions are necessary to specify the problem. The first condition is derived from the rear of the current:

$$u = 0, \quad \text{when} \quad h = D, \tag{13}$$

[2] The case of the rigid lid is considered.

and the second condition is derived from the front of the current:

$$u = F\sqrt{g'h}, \tag{14}$$

where F is a constant Froude number.

By adding (9) to (10) and subtracting (10) from (9), the governing equations are transformed into:

$$\{\partial_t + (u+c)\partial_x\}(u+2c) = 0, \tag{15}$$

$$\{\partial_t + (u-c)\partial_x\}(u-2c) = 0. \tag{16}$$

We solve this problem by using the method of characteristics. This method enables us to treat the PDE as an ODE. Characteristics are defined as $(t(s), x(s))$ where s is a parameter. Then the following relations are assumed:

$$\frac{dt}{ds} = 1, \quad \text{and} \quad \frac{dx}{ds} = u \pm c. \tag{17}$$

First, the case of positive characteristic (+ is chosen in (17)) is examined. Because of (15) and the following formula;

$$\frac{d}{ds} = \frac{\partial}{\partial t} + (u+c)\frac{\partial}{\partial x}, \tag{18}$$

$u + 2c$ is constant along the positive characteristic:

$$\frac{d(u+2c)}{ds} = 0. \tag{19}$$

By using the definition (17), the parameter s can be removed:

$$\frac{dx}{dt} = u + c. \tag{20}$$

The above equation describes the positive characteristic. In the same manner, $u - 2c$ is constant along the negative characteristic which is calculated by $\frac{dx}{dt} = u - c$.

Then we derive the specific solution of the situation shown in Figure 3. First, the case of $x < 0, t < 0$ is examined. From the initial conditions, $u = 0$ and $c = C := \sqrt{g'D}$. Then the characteristics are given by $\frac{dx}{dt} = \pm C$.

Second, the region of $x < 0, t > 0$ is examined. Here, there is a boundary line ($x = -Ct$) which represents the margin of the left propagating disturbance from the origin. So we have to consider separately the left and right regions from the boundary line. In the left region, by using the result of the region $x < 0, t < 0$, $u \pm 2c = \pm 2C$ along the positive and negative characteristics, respectively. Thus, $u = 0$ and $c = C$ holds in the left region from the boundary line.

On the other hand, in the right region, $u + 2c = 2C$ holds along the positive characteristics, and $u - 2c = A(\text{const})$ holds along the negative ones. At the origin, as there is a discontinuity of h in the initial condition, the wave speed can not be decided uniquely and then the negative characteristics intersect each other. From these equations, $2u = 2C + A$ and $c = \frac{2C-A}{4}$ hold. It is clear that the negative characteristics are straight lines, while the positive ones are curves due to the variation of A.

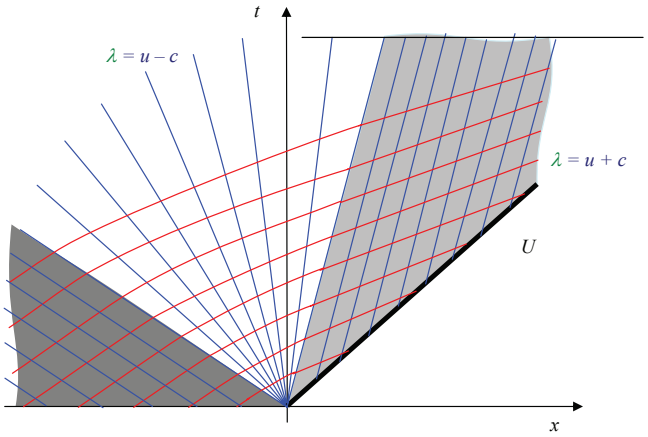

Figure 3: Characteristics for the problem of the gravity current. Positive (negative) characteristics are red (blue). The dark gray region corresponds to the left region from the boundary line which represents the margin of the left propagating disturbance from the origin. Figure kindly provided by Stuart Dalziel.

3.1 Front Velocity and Height

The front is initially at the origin and at rest. Then given that $u \pm 2c$ is conserved along the curve in equation (20), we may write:

$$u \pm 2c = u \pm 2\sqrt{g'h} = 0 \pm 2\sqrt{g'D} = \pm 2C,$$

where in this case $u = U$, the front velocity. We also know that $U = Fc$, and substituting c into the above equation gives:

$$U = \frac{2FC}{F+2}. \tag{21}$$

This is the solution for the front velocity, with the condition dependent on the choice of F.

The height of the front can also be determined based on the Froude number. This is calculated by substituting $U = cF$ into equation (21) giving:

$$cF = \frac{2FC}{F+2} \implies \sqrt{g'h_f}F = \frac{2F\sqrt{g'D}}{F+2},$$
$$\frac{h_f}{D} = \frac{4}{(F+2)^2}. \tag{22}$$

Again it is seen from equation (22) that the solution is dependant on the value of F. Figure 4 illustrates this further by providing the shape of the front for values of F from 1 to 3.

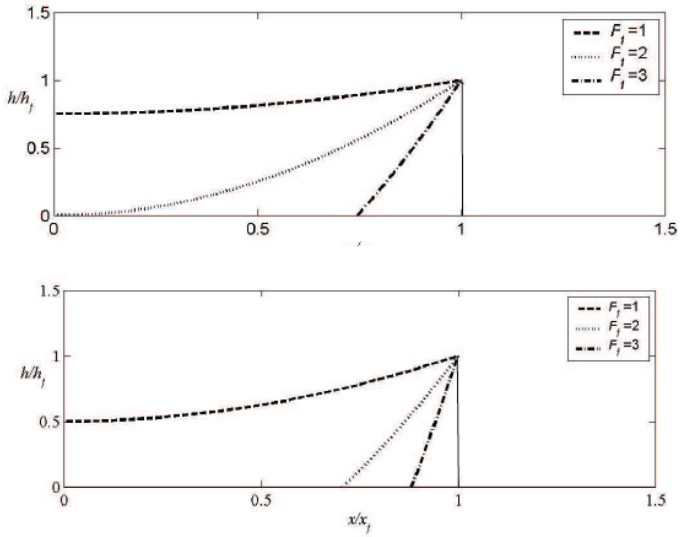

Figure 4: The shape of the front, x/x_f versus h/h_f, for varying values of the Froude number for both the channel (a) and axisymmetric current (b).

The full solution in the region $x > -Ct$ is given by the positive characteristic, $u + 2c = 2C$, and the negative characteristic, $\frac{dx}{dt} = u - c$, integrated to give $u - c = \frac{x}{t}$. Then solving these two equations simultaneously provides:

$$3c = 2C - \frac{x}{t} \implies 3\sqrt{g'h} = 2\sqrt{gD} - \frac{x}{t} \implies \sqrt{\frac{h}{D}} = \frac{2}{3} - \frac{x}{3Ct},$$

giving:

$$\frac{h}{D} = \frac{1}{9}(2 - \frac{x}{Ct})^2. \tag{23}$$

Equation (23) indicates the parabolic shape of the fluid height with x. We can also use this to obtain the position of the fluid by taking $h = h_f$ in (23) and equating this with (22) and rearranging:

$$\frac{x}{Ct} = \frac{2(F-1)}{F+2}. \tag{24}$$

Beyond the front position, the velocity and the depth remain constant as there is no fluid yet in this region, and this is indicated by the right hand non-shaded region in Figure 3.

The solutions provided above are clearly dependent on the value of F chosen. As an example, consider the case where $F = 1$ at time $Ct = 1$ shown in Figure 5. Substituting these values into equation (22), for an initial fluid depth $D = 1$, provides the front height as $h_f = 4/9$ and flow velocity $\frac{u}{C} = 2 - \frac{2c}{C} = \frac{2}{3}(1 + \frac{x}{Ct})$, which is indicated by the dashed line in the figure.

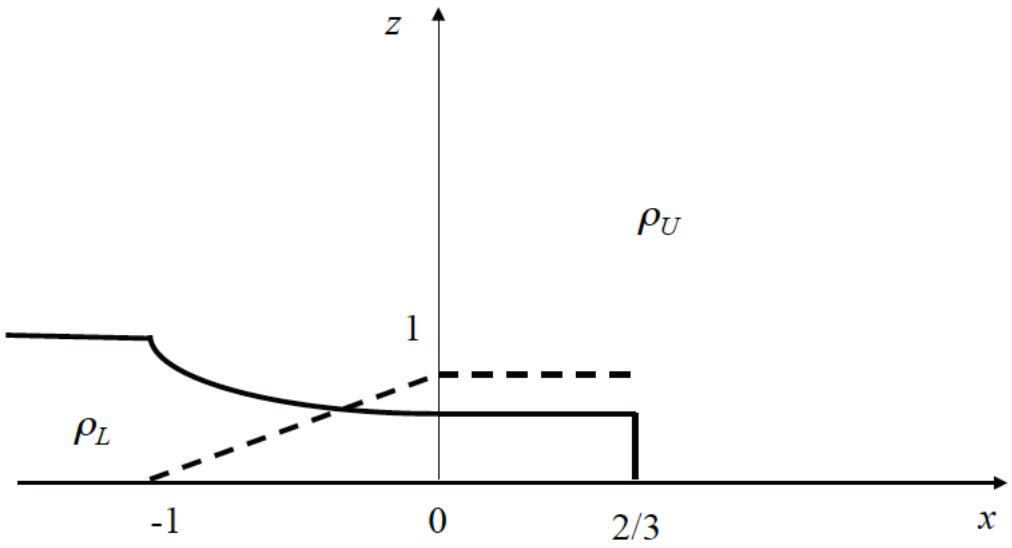

Figure 5: Distance versus height for the characteristic solution case of $Ct = 1$ and $F = 1$ showing the non dimensional depth of the fluid as the solid line and the non dimensional velocity as the dashed line.

3.2 Further Reading

For further reading on gravity currents, the reader is referred to the books and papers of John Simpson. His interest in the area was initiated from his time as a glider pilot, where he discovered the constant lift provided by uplifting sea breezes displaced by the lower outgoing land air that acted like a gravity current. His interest led to a number of books and influenced many to begin their own research in the area. As a couple of example references to his work, refer to [3], [4], [5] and [6].

4 Finite Volume Release

Consider now a one layer fluid, this time bounded in a finite volume (Figure 6).

We apply the same set of equations as previously, that is, the conservation of mass and momentum equations, and solve using dimensional analysis. The first step is to define the front velocity as:

$$u(x_f, t) = \dot{x_f}^2,$$

and apply the Froude condition:

$$F_f^2 g' h(x_f, t) = \dot{x_f}^2.$$

Now assuming conservation of volume (no mixing occurs within the system) we may write:

$$\int_0^{x_f} h(x, t) dx = V = DL_0.$$

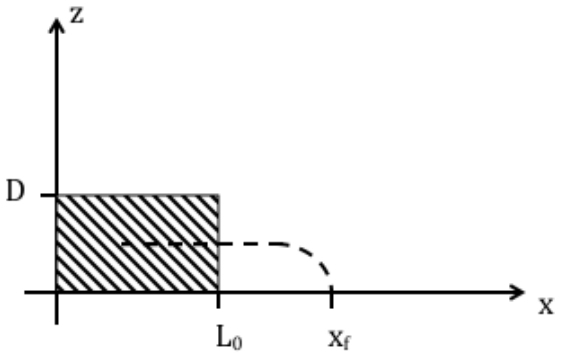

Figure 6: Two dimensional one layer fluid of finite volume, initial state (solid) and possible later state after lock release (dashed).

The flow can then seen to be defined by 5 governing parameters x, t, B, L_0 and F with two independent dimensions, length and time. Therefore, we make 3 dimensionless quantities and using the fact that $[B] = L^3T^{-2}$, define these quantities as:

$$\eta = \frac{x}{B^{\frac{1}{3}}t^{\frac{2}{3}}}, \qquad \tau = \frac{tB^{\frac{1}{2}}}{L_0^{\frac{3}{2}}}, \qquad F_f. \tag{25}$$

Applying dimensional analysis we therefore define:

$$u = \frac{x}{t}U(\eta, \tau, F_f), \tag{26}$$

$$g'h = \frac{x^2}{t^2}H(\eta, \tau, F_f), \tag{27}$$

$$x_f = xX(\eta, \tau, F_f), \tag{28}$$

where x_f is a function of x because the front velocity no longer travels at a constant speed with the finite volume case. We look for long time solutions, that is, solutions that are independent of the finite volume and so do not depend on L_0 (which is equivalent to saying the solution is independent of τ and so the above equations may be assumed to depend only on η and F). Applying the mass and momentum conservation equations in this situation we get:

$$\frac{\partial h}{\partial t} + \frac{\partial (uh)}{\partial x} = 0,$$

$$\frac{\partial}{\partial t}(\frac{x^2}{t^2}H) + \frac{\partial}{\partial x}(\frac{x^3}{t^3}UH) = 0,$$

$$-2\frac{x^2}{t^3}H + \frac{x^2}{t^2}\frac{\partial H}{\partial \tau}\frac{\partial \tau}{\partial t} + \frac{x^2}{t^2}\frac{\partial H}{\partial \eta}\frac{\partial \eta}{\partial t} + 3\frac{x^2}{t^3}UH + \frac{x^3}{t^3}\frac{\partial (UH)}{\partial \eta}\frac{\partial \eta}{\partial x}.$$

Since we've assumed the solution is now independent of τ then the $\frac{\partial H}{\partial \tau}$ goes to zero, and substituting $\frac{\partial \eta}{\partial x} = B^{-1/3}t^{-2/3}$ and $\frac{\partial \eta}{\partial t} = -\frac{2}{3}\frac{x}{B^{1/3}t^{5/3}}$ gives:

$$-2H - \frac{2}{3}H'\eta + 3UH + \eta(U'H + UH'),$$

which is rearranged and integrated:

$$\int \frac{dU}{U - \frac{2}{3}} = -\int \frac{dH}{H} - \int \frac{3}{\eta} d\eta,$$

providing:

$$U - \frac{2}{3} = \frac{k}{H\eta^3}, \tag{29}$$

where k is some constant of integration. Due to the conservation of the buoyancy, $g'h$ must always remain finite and so there is a discontinuity in (29) as x (and therefore η) approach zero. Hence, the only possible solution to (29) must be $k = 0$, producing the result $U = \frac{2}{3}$.

Now using conservation of momentum , equation (5), within the long time limit provides:

$$\frac{\partial}{\partial t}(\frac{x}{t}U) + \frac{x}{t}U\frac{\partial}{\partial x}(\frac{x}{t}U) = -\frac{\partial}{\partial x}(\frac{x^2}{t^2}H),$$
$$-\frac{x}{t^2}U + \frac{xU^2}{t^2} + \frac{Ux^2}{t^2}\frac{\partial U}{\partial \eta}\frac{\partial \eta}{\partial x} = -2\frac{x}{t^2}H - \frac{x^2}{t^2}\frac{\partial H}{\partial \eta}\frac{\partial \eta}{\partial x},$$

but since $U = \frac{2}{3}$ is a constant $\frac{\partial U}{\partial \eta} = 0$, then cancelling x and t terms and replacing with η we get:

$$\eta H' + 2H = U - U^2 = \frac{2}{9}. \tag{30}$$

Integrating equation (30):

$$H = \frac{1}{9} + \frac{K}{\eta^2}, \tag{31}$$

where K is a constant of integration. This the provides an expression for H where we must remove the unknown K term. To do, this return to the conservation of volume. Due to the constant g', conservation of buoyancy, which may be written as:

$$\int_0^{x_f} g'h(x,t)dx = B,$$

and:

$$\int_0^{x_f} g'h(x,t)dx = \int_0^{x_f} \frac{x^2}{t^2}Hdx = \int_0^{x_f} \frac{x^2}{t^2}(\frac{1}{9} + \frac{K}{\eta^2})dx.$$

Then replacing x with the equation for η the integral becomes:

$$x_f^3(\frac{1}{27} + \frac{K}{\eta_f^2}) = Bt^2. \tag{32}$$

Lastly we use the front condition on the Froude number:

$$u^2 = F^2 g' h \implies \dot{x_f^2} = F_f^2 g' h = F_f^2 \frac{x_f^2}{t^2} H = F_f^2 \frac{x_f^2}{t^2} (\frac{1}{9} + \frac{K}{\eta_f^2}),$$

and rearranging we can substitute the $K\eta_f^2$ term into (32) removing the K term and allowing the final governing equation to be found:

$$\dot{x_f^2} x_f = \frac{2}{27} F^2 \frac{x_f^3}{t^2} + F^2 B, \tag{33}$$

which has a solution of the form:

$$x_f = \Gamma t^{\frac{2}{3}}, \tag{34}$$

where $\Gamma = (\frac{27F^2B}{12-2F^2})^{\frac{1}{3}}$. The above results may also be put into dimensional terms:

$$x_f = (\frac{27F_f^2}{12 - 2F^2})^{\frac{1}{3}} B^{\frac{1}{3}} t^{\frac{2}{3}}, \tag{35}$$

$$\frac{h}{h_f} = 1 - \frac{1}{4} F^2 (1 - (\frac{x}{x_f})^2). \tag{36}$$

Hence, from the above results, it is found that the shape of the interface is parabolic in equation (36) and from equation (35) that the same $t^{\frac{2}{3}}$ time dependence occurs here as in the initial scaling analysis solution of the finite volume lock real case (the reader is referred to the second set of notes in this lecture series). Hence, we are seeing a similarity solution in each of the two cases. Figure 7 provides a comparison of the coefficient of the $t^{\frac{2}{3}}$ term in each case. In this figure, we see that as the Froude number is increased, the relative difference between the two solutions is also gradually increasing. Yet despite this difference, the insight given by the simplified box model still allows a result within approximately 20% of the shallow water model, displaying its usefulness as a tool for obtaining an approximate idea of the characteristics of the flow.

Figure 8 then provides the time evolution of the shape of the flow when initiated from a full depth lock. It is seen that after the initial sharp change, where the lock is released and there are large acceleration of the fluid, the head of the fluid flow remains at an approximately constant speed. At later times in the evolution this speed decelerates, as expected from the analysis and the similarity solution obtained. It is also noted that the head height reduces over time, this is due to the finite volume of the initial fluid and the flow left within the tail of current reduces the head volume.

Figure 9 shows the depth profiles for various similarity phases compared to the similarity solution case for three different Froude numbers. The similarity solutions do not extend to the furthest right of the profile at the front of the flow as the front region is very turbulent and the shallow water equations cannot be expected to represent this region. In the region prior to the front however, reasonable agreement can be observed between the theoretical and experimental cases with the larger value of the Froude number providing the closest agreement.

Looking also at the case of a partial depth release, Figure 10 indicates a longer, shallower tail region than in the full depth release case. This implies that a greater portion of the fluid

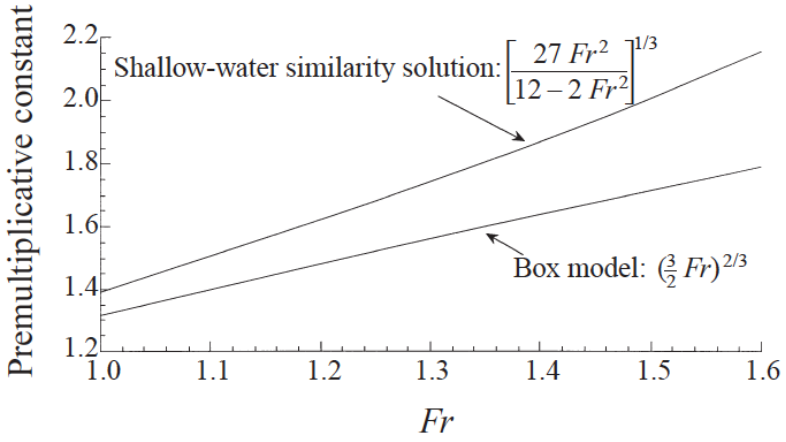

Figure 7: Coefficient of front distance for each of the cases in the similarity solution; the shallow water case derived in these notes and the box model in lecture two of this series.

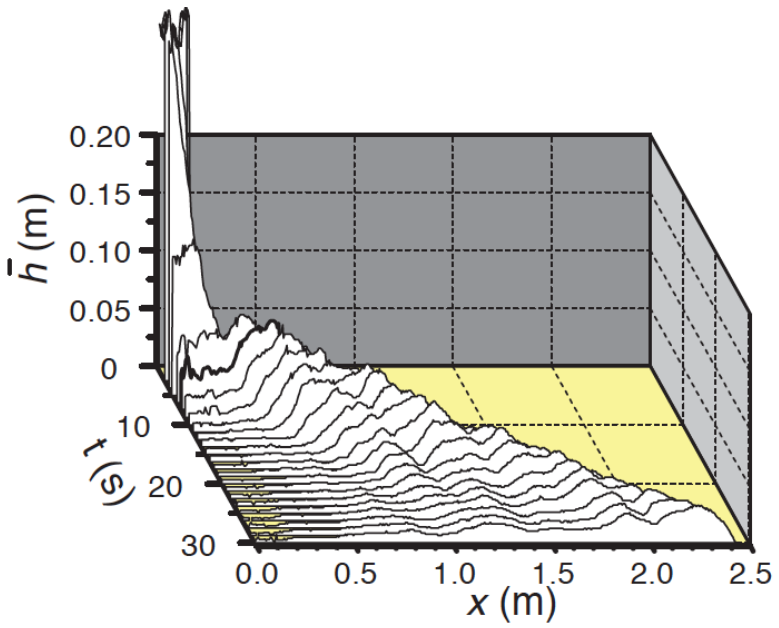

Figure 8: Height profiles at various stages of a full depth release flow with D/H=1 [1].

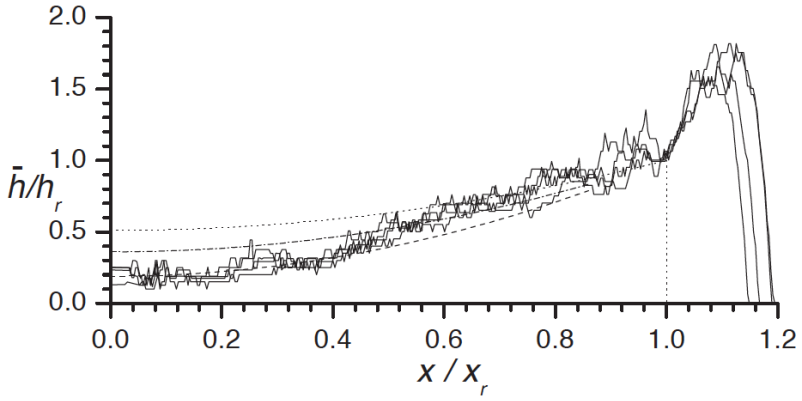

Figure 9: Equivalent height profiles for a full-depth with similarity phase values t/t_c =43.4, 46.9, 49.8 and 56.8. The profiles depicted by dotted, dash-dotted and dashed line profiles the similarity solutions to the shallow water equation for F_f =1.4, 1.6 and 1.8, respectively [1].

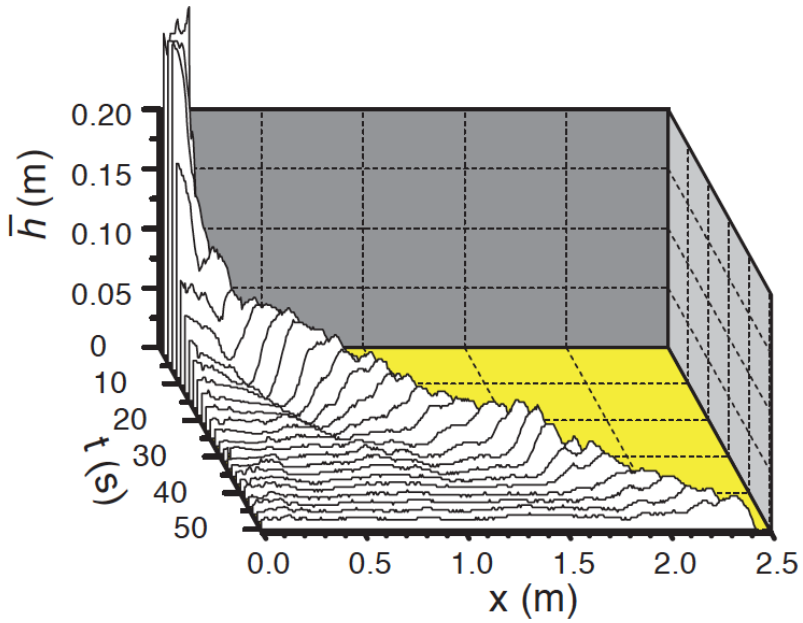

Figure 10: Height profiles at various stages of a partial depth release flow with D/H=0.675 [1].

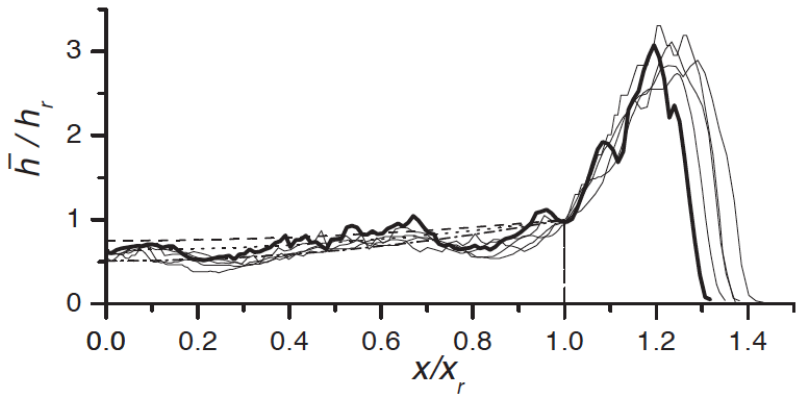

Figure 11: Equivalent height profiles for a partial-depth with similarity phase values t/t_c =43.4, 46.9, 49.8 and 56.8. The profiles depicted by dotted, dash-dotted and dashed line profiles the similarity solutions to the shallow water equation for F_f =1.4, 1.6 and 1.8, respectively [1].

is concentrated within the front region. The reader is referred to the paper of [2] for more details as here is provided an in depth analysis of the differences between the full and partial depth cases. In particular the main differences between the two cases can be attributed to the disturbances reflecting from the lock being closer to a bore case in higher initial depth locks and an expansion wave in shallower cases.

Figure 11 shows a comparison for the theoretical and experimental results of the similarity phase as in Figure 9 but now for the partial depth situation. Similar results are seen in this case as in Figure 9 with reasonable agreement between both sets of results, in particular when considering the error range of the experimental values.

Lastly lets consider alternatives for calculating the Froude number and where they are most relevant. Define F_D as the Froude number determined from the lock depth D; F_h as the Froude number evaluated from the maximum head height h and F_r as the Froude number determined from the height of the rear of the head. The definition of the rear of the head becomes rather difficult to precisely pin-point given the variation of profile shape over time and hence, as would be expected from such a definition, produces the greatest amount of scatter in the results (for full depth release see Figures 12 and partial depth release see Figure 13). Further, from the results in Figures 12 and 13, it is observed that the F_D definition provides the closest estimate to the constant velocity situation, where energy conserving theory may be applied, yet begins to diverge after the similarity phase is reached (this point is indicated by the vertical dashed lines). After the similarity phase, F_D decreases as expected for a Froude number defined in this manner. The F_h term however, remains fairly constant beyond the similarity phase, providing the best estimate of the speed in this region, despite the fact that it is derived from a non-hydrostatic region of the flow.

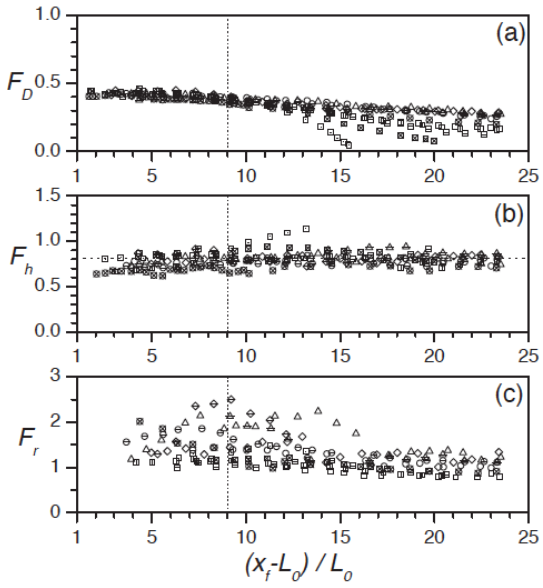

Figure 12: Evolution of the Froude number for the full-depth releases where F_f is determined from the lock height D, F_h from the maximum head height and F_r from the height of the rear of the head. The horizontal dashed line provides the average of the results while the vertical dashed lines indicates the area of departure from the constant-velocity phase situation. [1].

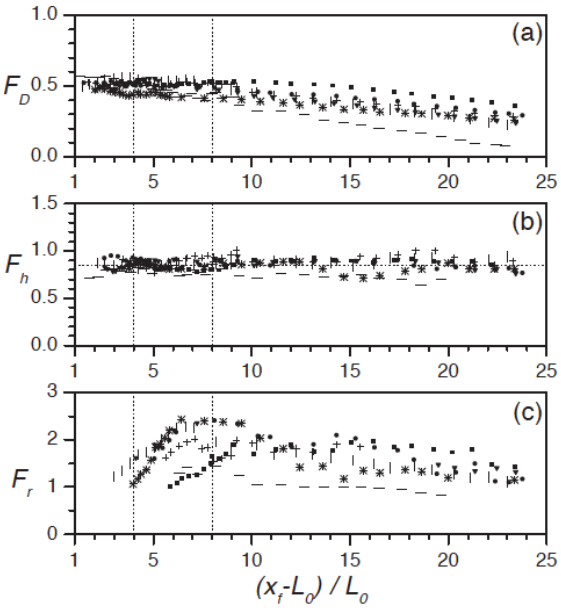

Figure 13: Evolution of the Froude number for the partial-depth releases where F_f is determined from the lock height D, F_h from the maximum head height and F_r from the height of the rear of the head. The horizontal dashed line provides the average of the results while the vertical dashed lines indicates the area of departure from the constant-velocity phase situation. [1].

References

[1] B. M. Marino, L. P. Thomas, and P. F. Linden, *The front condition for gravity currents*, J. Fluid Mech., 536 (2005), pp. 49–78.

[2] J. W. Rottman and J. E. Simpson, *Gravity currents produced by instantaneous release of a heavy fluid in a rectangular channel*, J. Fluid Mech., 135 (1983), pp. 95–110.

[3] J. E. Simpson, *A comparison between laboratory and atmospheric density currents*, Q. J. R. Met. Soc., 95 (1969), pp. 758–765.

[4] ——, *Effects of lower boundary on the head of a gravity current*, J. Fluid Mech., 53 (1972), pp. 759–768.

[5] ——, *Gravity currents in the environment and the laboratory*, Ellis Horwood, Chichester, 1987.

[6] ——, *Gravity Currents*, Cambridge University Press, 2nd ed., 1997.